

Thermal Decomposition of Quinoline and Isoquinoline. The Role of 1-Indene Imine Radical

Alexander Laskin[†] and Assa Lifshitz*

Department of Physical Chemistry, The Hebrew University, Jerusalem 91904, Israel

Received: September 12, 1997; In Final Form: November 13, 1997

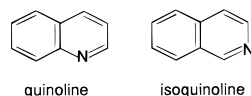
The thermal reactions of quinoline and isoquinoline were studied behind reflected shock waves in a pressurized driver single pulse shock tube over the temperature range 1275–1700 K and densities of $\sim 3 \times 10^{-5}$ mol/cm³. The decomposition products found in the postshock mixtures of quinoline and isoquinoline and their production rates were identical for both isomers. They were C₂H₂, C₆H₅CN, HC≡CCN, C₆H₆, HCN, C₆H₅–C≡CH, and C₄H₂. Trace quantities of C₆H₄, C₅H₅N and C₅H₄N–C≡CH were also found. The total disappearance rates of quinoline and isoquinoline are the same, and in terms of a first-order rate constant they are given by $k_{\text{total}} = 10^{13.0} \exp(-75.5 \times 10^3/RT) \text{ s}^{-1}$ where R is expressed in units of cal/(K mol). The same product distribution in the two isomers can be accounted for if the production of 1-indene imine radical as an intermediate is assumed. A kinetic scheme containing the reactions of both quinoline and isoquinoline with 72 species and 148 elementary reactions accounts for the observed product distribution. The reaction scheme is given, and the results of computer simulation and sensitivity analysis are shown.

I. Introduction

The present investigation on the decomposition of quinoline and isoquinoline is a continuation of our investigation on the decomposition of nitrogen containing aromatic compounds. It is well-known^{1–3} that fuel nitrogen in coal is predominantly pyrrole and pyridine type nitrogen, with a slightly higher weight to compounds containing the pyrrole ring.³ The study of the pyrolysis of benzopyrrole (indole) and benzopyridine (quinoline) as the basic nitrogen containing components of the coal matrix is an important element in the understanding coal combustion.

We have recently published a detailed investigation of the thermal reactions of indole.⁴ These reactions were found to be similar to those of pyrrole, and as far as the reactions of the pyrrole ring are concerned, they could be predicted from the mechanism of the pyrolysis of pyrrole.^{5,6} The thermal reactions of indole are mostly isomerizations at low temperatures (low conversions) and as the temperature increases fragmentations take over. The assumption of the existence of an indole ↔ indolenine tautomerism was necessary to explain the production of the isomerization products.

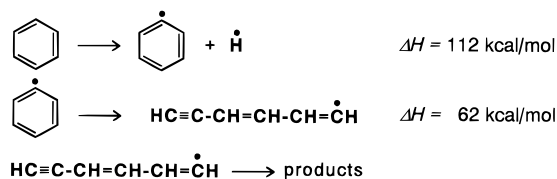
In the present article, we report on a study of the pyrolysis of quinoline and isoquinoline. Both molecules contain a pyridine ring fused to benzene. The nitrogen atom occupies an α -position in quinoline and a β -position in isoquinoline. Both molecules have approximately the same thermal stability, their standard heats of formation⁷ being 52.2 and 50.2 kcal/mol, respectively.



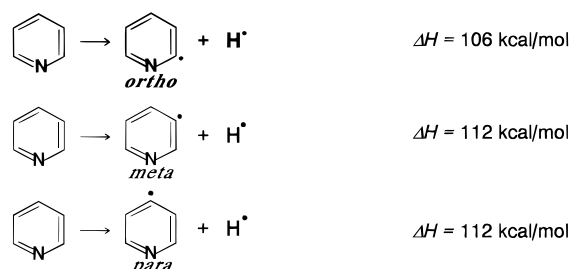
We are aware of only one study on the thermal decomposition of quinoline, by Bruinsma et al.,⁸ who reported on its overall decomposition rate and its Arrhenius parameters. No data on the distribution of reaction products or on the decomposition

mechanism were given. The thermal decompositions of benzene and pyridine, on the other hand, have been extensively studied, discussed, and summarized.^{9–11} They are essential for interpreting the results of the present investigation.

The initiation step in the thermal decomposition of benzene involves an ejection of a hydrogen atom from one of the six C–H bonds in the molecule, forming phenyl radical and a hydrogen atom.^{9,11} The fragmentation of the phenyl radical is preceded by a β -scission of the ring forming a linear chain *l*-C₆H₅[•] radical. This radical decomposes via several reaction channels yielding mainly C₂H₂ and C₄H₂ as final products.

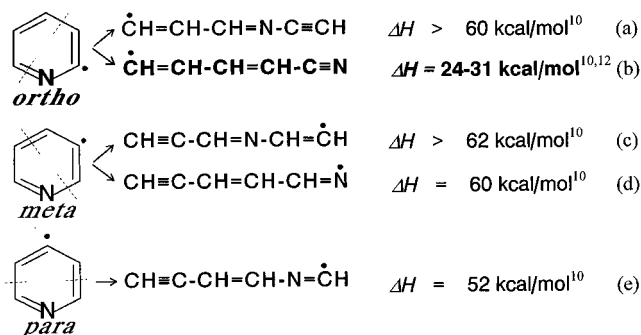


The mechanism of pyridine decomposition is very similar to that of benzene. It is somewhat more complicated, however, owing to the decreased symmetry in pyridine as compared to benzene. As a result of the H-atom ejection from the pyridine ring, ortho, meta, and para pyridyl radicals can be formed. The thermochemistry of the pyridyl radicals shows that the production of ortho pyridyl radical is preferred, owing to its stabilization by the neighboring nitrogen. Ab initio calculations¹² give a value of 6 kcal/mol for the stabilization energy.



[†] In partial fulfillment of the requirement of a Ph.D. Thesis to be submitted to the Senate of the Hebrew University of Jerusalem by A. Laskin.

The β -scissions of the various pyridyl radicals lead to five different open ring structures with different locations of the nitrogen in the open chain. The thermochemistry of the β -scission of the ortho radical is quite different from those of the meta and para radicals. Out of the five possible β -scission channels only one forms the strong $\text{C}\equiv\text{N}$ bond. This is the C–N bond scission in the ortho pyridyl radical (channel b). This scission makes the open-chain radical much more stable than all other radicals obtained from the meta and para pyridyls.



Therefore, the formation of the ortho pyridyl radical in the first step, as well as the β -scission of its C–N bond in the second step, is the preferred pathway for pyridine decomposition. The decomposition of the open chain cyano radical leads mainly to the production of C_2H_2 and $\text{HC}\equiv\text{CCN}$.

Since quinoline and isoquinoline are built from these two rings, it is reasonable to assume that similar reaction pathways operate in their thermal decompositions. In this report we describe the thermal reactions of quinoline and isoquinoline, compose a reaction scheme for the overall decomposition and describe the results of computer simulations that support the suggested mechanism. It will be shown that the product distribution can be accounted for only if production of 1-indene imine radical as an intermediate is assumed.

The thermal reactions of quinoline and isoquinoline are initiated by an H-atom ejection from the pyridine ring. In both molecules the H atom in the ortho position to the nitrogen is the preferred ejection site owing to the resonance stabilization of the remaining radical. It will be shown later that, following the preferred β -scission of the C–N bond, the main decomposition products in quinoline are expected to be $\text{HC}\equiv\text{CCN}$ and C_6H_6 and in isoquinoline C_2H_2 and $\text{C}_6\text{H}_5\text{CN}$. However, the experimental results show that the concentrations of all the decomposition products are absolutely the same irrespective of whether the original reactant is quinoline or isoquinoline. To describe this fact we assume the existence of 1-indene imine radical intermediate which plays the central role in the thermal decomposition of quinoline and isoquinoline.

II. Experimental Section

Apparatus. The thermal decompositions of quinoline and isoquinoline were studied behind reflected shocks in a pressurized driver, 52-mm i.d. single-pulse shock tube made of Double Tough Pyrex tubing. The tube and its gas-handling system were maintained at $150 \pm 1^\circ\text{C}$ with a heating system with 15 independent computer-controlled heating elements.

The shock tube had a 4-m long driven section divided in the middle by a 52-mm i.d. ball valve. The driver section had a variable length up to a maximum of 2.7 m and could be varied in small steps in order to obtain the best cooling conditions. Cooling rates were approximately $5 \times 10^5 \text{ K/s}$. A 36-L dump

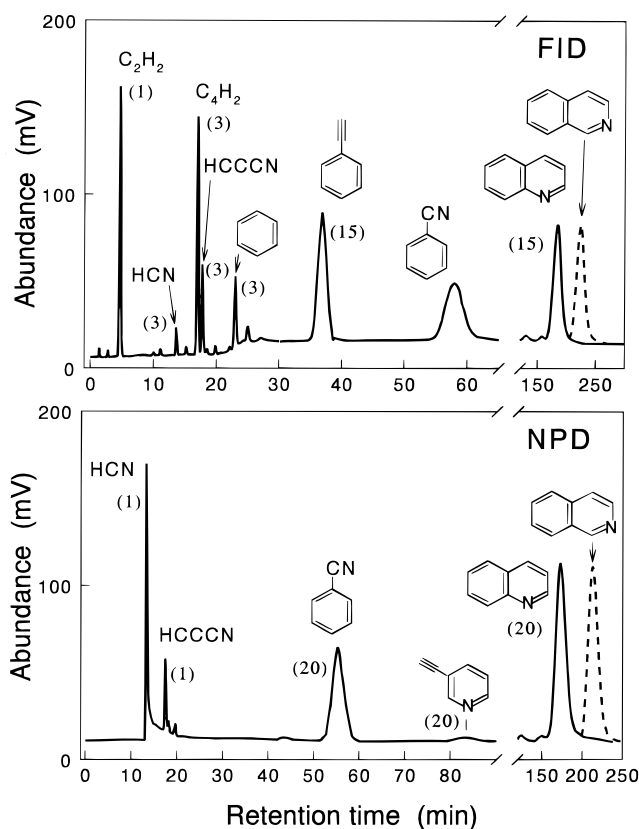


Figure 1. Gas chromatograms of a postshock mixture of 0.3% quinoline in argon heated to 1590 K, taken with FID and NPD. Isoquinoline is absent from the products. The broken-line peak shows its retention time on the column relative to quinoline. The numbers in parentheses indicate multiplication factors.

tank was connected to the driven section at 45° angle toward the driver near the diaphragm holder in order to prevent reflection of transmitted shocks and in order to reduce the final pressure in the tube. The driven section was separated from the driver by Mylar polyester films of various thickness depending upon the desired shock strength.

Prior to performing an experiment, the tube and the gas-handling system were pumped down to $\sim 3 \times 10^{-5}$ torr. The reaction mixtures were introduced into the driven section between the ball valve and the end plate, and pure argon was introduced into the section between the diaphragm and the valve, including the dump tank. After each experiment a gas sample was transferred from the tube through a heated injection system to a Hewlett-Packard model 5890A gas chromatograph operating with flame ionization (FID) and nitrogen phosphor (NPD) detectors.

The temperatures and densities of the gas behind the reflected shocks were calculated from the measured incident shock velocities using the three conservation equations and the ideal gas equation of state. The molar enthalpies of quinoline and isoquinoline were taken from the NIST-Structures and Properties Code.⁷ Incident shock velocities were measured with two miniature high-frequency pressure transducers (P. C. B. model 113A26) located 230 mm apart near the end plate of the driven section. The signals generated by the shock wave passing over the transducers were fed through an amplifier to a Nicolet model 3091 digital oscilloscope. Time intervals between the two signals shown on the oscilloscope were obtained digitally with an accuracy of 2 ms, corresponding to approximately 20 K. A third transducer placed in the center of the end plate provided

TABLE 1: Experimental Conditions and Product Distribution in Postshock Mixtures of Quinoline^a

T_5 (K)	dwelt time (ms)	$C_5 \times 10^5/\text{cm}^3$	quinoline	C_2H_2	$\text{C}_6\text{H}_5\text{-CN}$	$\text{HC}\equiv\text{CCN}$	C_6H_6	HCN	$\text{C}_6\text{H}_5\text{C}\equiv\text{CH}$	C_4H_2
1290	2.00	2.50	99.29	0.45	0.15	0.029		0.021	0.059	
1295	1.96	2.56	99.46	0.31	0.13	0.018	0.016	0.011		0.053
1310	2.02	2.31	99.20	0.42	0.18	0.023	0.048	0.030	0.10	
1320	2.03	2.49	99.14	0.45	0.22	0.030	0.033	0.056	0.072	
1325	2.02	2.30	99.03	0.52	0.22	0.036	0.043	0.046	0.073	0.033
1335	2.00	2.45	98.48	0.85	0.27	0.10	0.073	0.041	0.14	0.038
1335	2.00	2.56	98.23	0.89	0.34	0.15	0.070	0.061	0.14	0.065
1362	2.04	2.57	98.07	1.00	0.41	0.083	0.081	0.13	0.19	0.154
1365	2.00	2.45	97.42	1.38	0.40	0.16	0.094	0.18	0.19	0.166
1385	2.00	2.40	97.71	1.34	0.38	0.12	0.15	0.06	0.15	0.085
1385	2.00	2.59	97.15	1.54	0.46	0.16	0.12	0.21	0.22	0.13
1410	2.00	2.40	93.28	3.35	1.15	0.34	0.34	0.60	0.52	0.41
1410	1.99	2.27	86.05	6.72	1.49	0.74	0.61	1.98	1.01	1.42
1415	2.0	2.33	94.62	2.92	0.75	0.28	0.31	0.18	0.47	0.48
1445	2.00	2.37	90.46	4.47	1.24	0.61	0.37	1.08	0.66	1.11
1457	1.94	2.53	91.13	3.79	1.36	0.35	0.38	1.48	0.66	0.86
1465	2.00	2.37	87.10	6.43	1.31	0.85	0.52	1.29	0.84	1.65
1490	2.00	2.53	77.77	10.00	1.95	1.11	0.72	3.52	0.90	4.02
1490	2.00	2.45	77.20	11.10	1.71	1.40	0.92	2.41	1.23	4.03
1500	1.99	2.18	71.22	12.41	2.72	1.55	1.15	5.23	1.71	4.00
1500	1.96	2.12	66.77	14.21	2.88	1.68	1.37	6.38	1.99	4.70
1535	2.00	2.25	68.89	13.65	2.34	2.15	1.14	5.41	1.39	5.05
1550	1.96	2.20	52.66	20.87	3.96	2.27	1.68	9.67	1.87	7.02
1550	1.93	2.15	39.99	28.17	4.32	2.55	2.11	10.43	2.50	9.93
1565	1.95	2.25	39.94	24.76	3.91	2.66	1.79	12.90	1.65	10.77
1570	1.99	2.07	23.94	33.57	3.37	4.22	1.75	16.37	1.67	15.10
1607	1.96	2.14	16.65	46.29	2.98	3.23	1.87	18.57	1.27	9.14
1650	1.98	2.09	12.85	44.00	2.16	2.75	1.92	19.30	0.92	16.09

^a In mole percent. H_2 , C_6H_4 , $\text{C}_5\text{H}_5\text{N}$, and $\text{C}_5\text{H}_4\text{N-C}\equiv\text{CH}$ are not included in the table.

measurements of the reaction dwell time (approximately 2 ms) with an accuracy of $\pm 5\%$.

Materials and Analysis. Reaction mixtures containing 0.3% quinoline (or isoquinoline) diluted in argon, were prepared in 12 L glass bulbs and stored at 150 ± 1 °C and 700 torr. Both the bulbs and the line were pumped down to approximately 10^{-5} torr before the preparation of the mixtures. 2.1 torr (0.3% of 700 torr) of quinoline or isoquinoline in the gas phase correspond approximately to 5% of their equilibrium vapor pressure at 150 °C, so that wall condensation is negligible. Quinoline, listed as 98.0% pure, and isoquinoline, 97.0% pure, were obtained from Aldrich Chemical Co. Each showed only one GC peak. The argon used was Matheson ultrahigh purity grade, listed as 99.9995%, and the helium was Matheson pure grade, listed as 99.999%. All materials were used without further purification.

Gas chromatographic analyses of the postshock mixtures were performed on two 1-m Porapak N columns with flame ionization and nitrogen phosphor detectors. Identification of reaction products was based on their GC retention times assisted by a Hewlett-Packard model 5970 mass selective detector. Typical FID and NPD chromatograms of a mixture containing 0.3% quinoline in argon, shock-heated to 1520 K, are shown in Figure 1.

The concentrations of the reaction products $C_5(\text{pr}_i)$ were calculated from their GC peak areas using the relations:¹³

$$C_5(\text{pr}_i) = A(\text{pr}_i)/S_5(\text{pr}_i) \times \{C_5(\text{reactant})_0/A(\text{reactant})_0\} \quad (1)$$

$$C_5(\text{reactant})_0 = p_1\{\%(\text{reactant})\rho_5/\rho_1\}/100RT_1 \quad (2)$$

$$A(\text{reactant})_0 = A(\text{reactant})_i + (1/9) \times \sum N(\text{pr}_i)A(\text{pr}_i)/S(\text{pr}_i) \quad (3)$$

In these relations, $C_5(\text{reactant})_0$ is the concentration of quinoline or isoquinoline behind the reflected shock prior to decomposition and $A(\text{reactant})_0$ is their calculated GC peak area

prior to decomposition (eq 3) where $A(\text{pr}_i)_i$ is the peak area of a product i in the shocked sample, $S(\text{pr}_i)$ is its sensitivity relative to that of the reactant, $N(\text{pr}_i)$ is the number of its carbon atoms, ρ_5/ρ_1 is the compression behind the reflected shock, and T_1 is the initial temperature, which was 423 K in the present series of experiments.

The FID and NPD sensitivities of the products relative to the reactant were determined from standard mixtures. They were estimated for C_4H_2 , $\text{HC}\equiv\text{C-CN}$, and $\text{C}_5\text{H}_4\text{N-C}\equiv\text{CH}$, based on comparisons to the relative sensitivities of similar compounds. GC peak areas were recorded with a Spectra Physics model SP4200 computing integrator and transferred after each analysis to a PC for data reduction and graphical presentation.

III. Results

In order to determine the product distribution in the thermal decompositions of quinoline and isoquinoline, some 30 experiments were carried out with quinoline as a reactant molecule and 20 with isoquinoline. The temperature range covered in these experiments was 1275–1700 K at overall densities behind the reflected shock wave of $\sim 3 \times 10^{-5}$ mol/cm³.

Details of the experimental conditions and the product distribution are given in Tables 1 and 2 for quinoline and isoquinoline, respectively. The mole percents given in the tables correspond to those of the products in the postshock mixtures irrespective of the number of their carbon atoms. Molecular hydrogen was not measured and was not included in the tables.

The decomposition products found in the postshock mixtures were identical in the two series of experiments, both in distribution and production rates. No quinoline \leftrightarrow isoquinoline isomerization occurred. Neither traces of isoquinoline in shock-heated mixtures of quinoline nor traces of quinoline in shock-heated mixtures of isoquinoline were found. In both series, GC analyses revealed the presence of C_2H_2 , $\text{C}_6\text{H}_5\text{-CN}$, $\text{HC}\equiv\text{C-CN}$, C_6H_6 , HCN, $\text{C}_6\text{H}_5\text{-C}\equiv\text{CH}$, and C_4H_2 as major decomposi-

TABLE 2: Experimental Conditions and Product Distribution in Postshock Mixtures of Isoquinoline^a

T_5 (K)	dwelt time (ms)	$C_5 \times 10^{-5}$ mol/cm ³	isoquinoline	C ₂ H ₂	C ₆ H ₅ -CN	HC≡CCN	C ₆ H ₆	HCN	C ₆ H ₅ -C≡CH	C ₄ H ₂
1275	2.00	2.48	99.56	0.23	0.075	0.012	0.033	0.021	0.065	
1300	2.04	2.62	99.09	0.48	0.12	0.040	0.060	0.055	0.14	
1335	2.03	2.73	98.06	1.01	0.25	0.087	0.12	0.11	0.29	0.057
1345	2.00	2.65	97.90	1.04	0.30	0.11	0.12	0.12	0.32	0.067
1360	2.04	2.38	98.06	0.94	0.27	0.095	0.10	0.13	0.32	0.079
1365	2.04	2.58	97.05	1.52	0.35	0.16	0.15	0.25	0.39	0.11
1365	2.01	2.50	96.96	1.42	0.36	0.17	0.16	0.32	0.45	0.15
1400	2.00	2.51	91.01	3.58	1.21	0.55	0.42	0.82	1.11	0.41
1415	2.00	2.33	89.01	5.21	1.22	0.72	0.55	0.94	1.51	0.84
1440	2.00	2.34	89.95	4.51	1.02	0.65	0.49	1.30	1.16	0.93
1460	2.00	2.30	89.74	4.53	1.02	0.70	0.50	1.31	1.08	1.11
1465	1.99	2.28	78.28	9.31	1.93	1.63	0.94	3.52	2.08	2.31
1480	2.00	2.26	79.70	8.04	1.66	1.68	0.91	4.12	1.72	2.15
1490	1.99	2.25	76.62	9.85	2.29	1.57	1.28	3.44	2.28	2.67
1505	1.99	2.10	66.25	13.10	2.87	2.27	1.60	7.43	2.72	3.75
1515	1.98	2.37	61.12	16.38	3.27	2.68	1.52	7.26	3.20	4.57
1550	1.99	1.97	56.02	17.16	2.92	2.99	1.66	11.73	2.27	5.24
1590	2.00	2.28	30.80	25.59	4.01	4.98	2.12	20.21	2.85	9.44
1600	1.98	2.53	26.21	27.25	4.74	4.78	2.72	20.51	3.40	10.39
1600	1.99	2.57	22.34	30.60	4.87	4.77	2.60	22.09	2.53	10.19
1630	1.98	2.23	22.53	29.74	3.56	5.40	2.08	23.22	2.32	11.15
1675	1.97	2.14	17.62	34.58	2.20	4.93	1.66	25.66	1.17	12.23
1700	1.98	2.00	12.47	37.82	2.06	5.02	1.39	22.01	1.10	18.12

^a In mole percent. H₂, C₆H₄, C₅H₅N, and C₅H₄N-C≡CH are not included in the table.

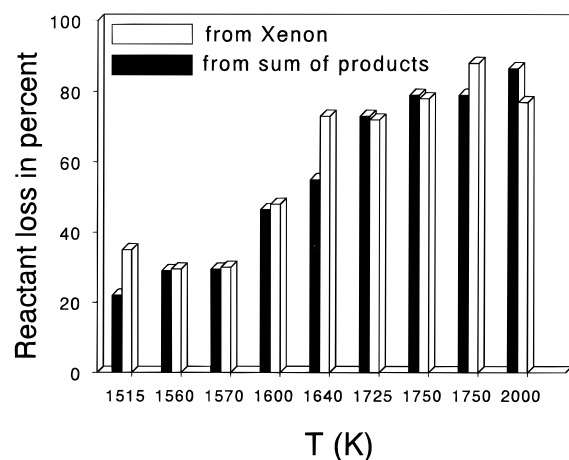


Figure 2. Recovery of reaction products tested in several runs with quinoline against the reactant loss, using 0.3% xenon in mixtures containing 0.3% quinoline in argon as an internal standard.

tion products. Trace quantities of C₆H₄, C₅H₅N, and C₅H₄N-C≡CH were also found in the postshock mixtures, particularly in high-temperature shocks.

The possible loss of products by adsorption on the shock tube walls or in the gas chromatograph was examined in the following manner. In several tests, 0.3% xenon was added to the reaction mixture and ratios [quinoline]/[xenon] were measured by GC-MS (using 30 cm Porapak N columns) in the unshocked and in several shocked samples. By comparing these ratios in the shocked and the unshocked samples, we could determine the relative loss of the reactant in each test. This relative loss was compared to the corresponding values calculated by the sum $(1/9)\sum N(\text{pr}_i)A(\text{pr}_i)/S(\text{pr}_i)$, which represents the concentrations of all the products normalized by the number of their carbon atoms (see Experimental Section, eq 3). These comparisons are shown graphically in Figure 2. Except for two tests, the ratios are practically the same, showing scatter in both directions. It seems therefore that there is no significant loss of products in the analyses.

The mass balance of nitrogen vs carbon is shown in Figure 3. The concentrations of the nitrogen containing species are plotted against one-ninth of the sum of the concentrations of

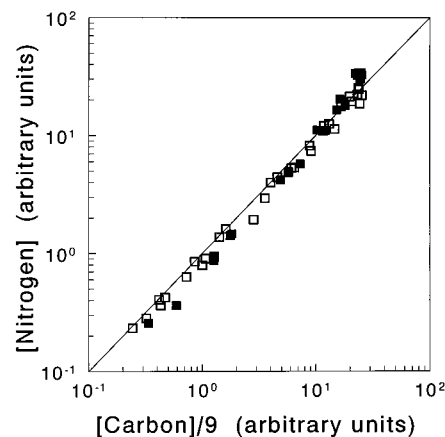


Figure 3. Nitrogen-carbon mass balance among the decomposition products. □, quinoline; ■, isoquinoline.

all the decomposition products, each multiplied by the number of its carbon atoms. The 45° line in the figure represents a complete nitrogen-carbon mass balance. As can be seen, within the limit of the experimental scatter, there is no significant deviation from a complete mass balance.

Figure 4 shows an Arrhenius plot of the overall decomposition of quinoline and isoquinoline calculated as first-order rate constants from the relation

$$k_{\text{total}} = -\ln([reactant]_t/[reactant]_0)/t \quad (4)$$

As can be seen the rates for quinoline and isoquinoline are practically the same. The value obtained (for the two molecules) is $k_{\text{total}} = 10^{13.0} \exp(-75.5 \times 10^3/RT) \text{ s}^{-1}$ where R is expressed in units of cal/(K mol). The value obtained by Bruinsma et al.⁸ for the total decomposition of quinoline in a low-temperature study is also shown for comparison. There is a good agreement between the values of the rate constants in the two studies on the basis of an extrapolation of the low-temperature data to the data of the present high-temperature study.

IV. Discussion

1. Reaction Mechanism. A. *Formation of Quinolyl and Isoquinolyl Radicals.* Similar to other aromatic systems, it is

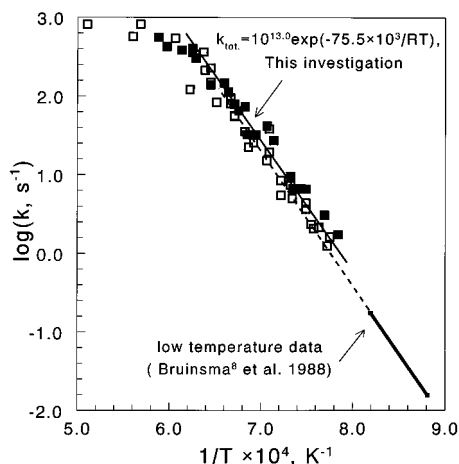
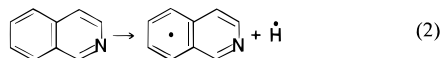
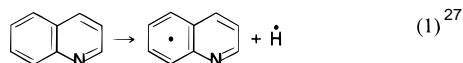


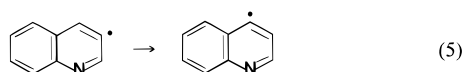
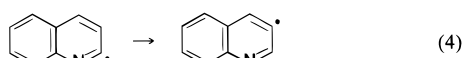
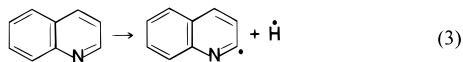
Figure 4. First-order Arrhenius plot of the overall decomposition of quinoline and isoquinoline. \square and broken line, quinoline; \blacksquare and solid line, isoquinoline. The low-temperature rate constant ($k_{\text{total}} = 10^{13.2} \exp(-77.9 \times 10^3/RT)$, s^{-1}) obtained by Bruinsma et al.⁸ is shown for comparison.

assumed here too that the initiation step in the thermal decompositions of quinoline and isoquinoline involves ejection of a hydrogen atom from the reactant by C–H bond cleavage. There are seven such bonds in each molecule, three in the pyridine ring, and four in the benzene ring. Thus, seven different radicals can in be formed as a result of H-atom ejection from each molecule. Each one can then decompose via its own decomposition pathway.

To simplify the overall decomposition mechanism and reduce the number of elementary reactions in the final kinetic scheme, we made two assumptions: 1. Since all four hydrogen atoms on the benzene ring are bound with the same bond energy (~ 112 kcal/mol), we have used only one radical in the benzene ring instead of four.

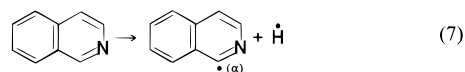
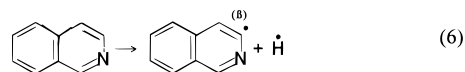


2. Meta and para quinolinyl radicals in the pyridine ring are less stable than the ortho radical and should therefore be considered as separate entities. However, to reduce the number of elementary reactions that produce these radicals, particularly abstraction reactions, we assumed that the only radical formed either by H-atom ejection or abstraction is the ortho quinolinyl radical, which then quickly equilibrates with the meta and para radicals.

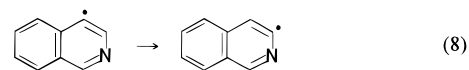


Note that reactions 4 and 5 are not necessarily elementary reactions. They simply provide a means to form the meta and the para radicals as if they were formed by H-atom ejection or abstraction.

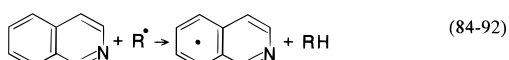
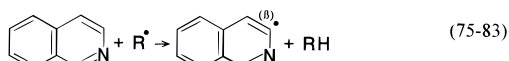
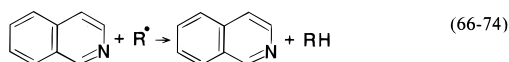
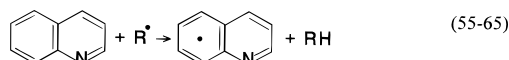
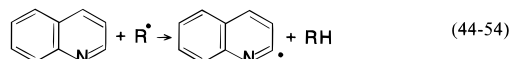
Similar representations were introduced for the isoquinolinyl radicals. The α -ortho and β -ortho isoquinolinyl radicals are considered to form by H-atom ejection or abstraction.



The meta isoquinolinyl radical in the pyridine ring then forms from the β -ortho isoquinolinyl radical by fast equilibration.

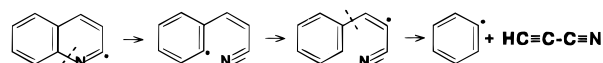


Quinolinyl and isoquinolinyl radicals result also from H-atom abstractions. At relatively low temperatures, H atoms are abstracted mainly by other hydrogen atoms. As the temperature increases and the concentrations of additional radicals in the system build up, hydrogen atoms are also abstracted by less reactive radicals such as $\text{C}_6\text{H}_5^\bullet$, $\text{C}_6\text{H}_4\text{CN}^\bullet$, $\text{C}_5\text{H}_4\text{N}^\bullet$, and others. H-atom abstractions by different radicals (R^\bullet) were introduced into the reaction scheme according to our formalism by forming two quinolinyl and three isoquinolinyl radicals. Forty nine such abstractions appear in the reaction scheme.



B. Preferred Decomposition Pathways. It has already been noted in the Introduction that the preferred pathway for the decomposition of the pyridine ring involves a H-atom ejection from the ortho position followed by β -scission of the C–N bond in the pyridyl radical.

In quinoline there is only one ortho site from which a H atom can be ejected. The preferred β -scission is the rupture of the C–N bond, similar to the process in pyridine. This leads to an open-chain radical, for which the further decomposition pathway of the lowest energy is a 1,4 H-atom migration in the first step and the formation of $\text{C}_6\text{H}_5^\bullet$ and $\text{HC}\equiv\text{CCN}$ in the second step.



Isoquinoline has two ortho positions with respect to the benzene ring, α and β (see reactions 6 and 7). Both are subjected to β -scission of the C–N bond. However, in contradistinction to the β -scission in the α -ortho radical, which opens without affecting the benzene ring, the β -scission of the C–N bond in the β -ortho radical results in the formation of a

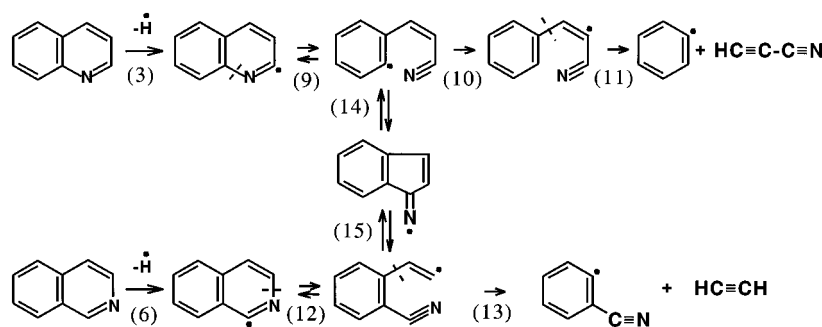


Figure 5. The reaction scheme showing the coupling between quinoline and isoquinoline in the "preferred pathways". Numbers in parentheses indicate reaction numbers as they appear in the reaction scheme.

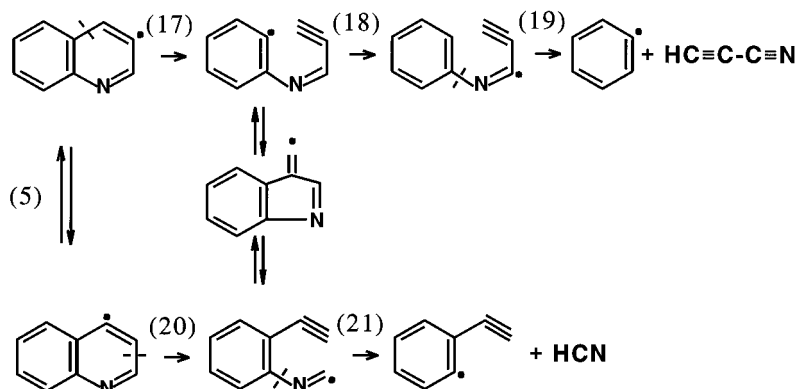
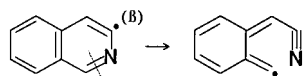
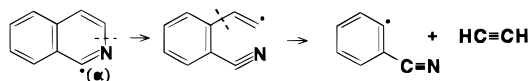


Figure 6. The reaction scheme showing the coupling between para and meta quinolyl and their reaction products. Numbers in parentheses indicate reaction numbers as they appear in the reaction scheme.

C=C bond conjugated to the benzene ring. It fixes the bonds in the benzene ring and destroys its aromaticity.



This process requires ~ 20 kcal/mol (AM1 estimation) more than the β -scission of the C–N bond in the α -ortho isoquinolyl radical. It appears that the preferred pathway for isoquinoline decomposition involves the α -ortho radical rather than the b . Its decomposition begins with a H-atom ejection from the α -ortho position in the pyridine ring, followed by β -scission of the C–N bond and decomposition of the open-chain radical to produce C_2H_2 and $C_6H_4CN^\bullet$.

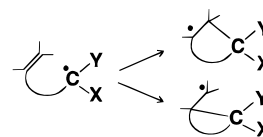


The $C_6H_5^\bullet$ and $C_6H_4CN^\bullet$ radicals are stable enough^{9,14} to be able to abstract or recombine with a hydrogen atom before decomposing.

The direct outcome of this analysis is that the preferred decomposition pathways of the two isomers yield different final products, $HC\equiv CCN$ and C_6H_6 in quinoline and C_2H_2 and C_6H_5-CN in isoquinoline.

There is clear experimental evidence, however, not only that the relative product abundances in the two isomers are identical, but also that the production rates of all the products are exactly the same, regardless of whether the reactant is quinoline or isoquinoline. This "discrepancy" could be accounted for if a very fast quinoline \leftrightarrow isoquinoline isomerization would take place. However, such an isomerization was not evident. No isomerization products were identified in postshock mixtures.

There must be a fast coupling between quinoline and isoquinoline reactions along their preferred pathways at early stages, before ring fragmentation occurs. This coupling equilibrates the open chain radicals in the two pathways so that they lose their identity. The coupling suggested in Figure 5 is based on the well-known¹⁵ phenomenon that open-chain radicals having π -bond in the chain undergo very fast radical-induced cyclization forming two possible cyclic structures:



In the present case the open-chain ortho quinolyl and α -ortho isoquinolyl radicals undergo cyclization to yield the same intermediate, namely, 1-indene imine radical.

Out of the two possible cyclizations in each one of the of the open-chain radicals, one is simply the back reaction of the opening of the ortho quinolyl and α -ortho isoquinolyl radicals and the other is the formation of indene imine radical. Once the latter has been formed, it can undergo two β -scissions to yield the two different open-chain radicals.

Since the nitrogen is *outside* the five-membered ring, the β -scission location determines whether the product of the decyclization is a member of the quinoline or isoquinoline pathway.

C. Additional Radical Decomposition Pathways. Figure 6 shows the ring cleavage of meta and para quinolyl and the consequent fragmentation of the open-chain radicals. The overall decomposition pathways were constructed in such a way that both the ring opening and the fragmentation would follow the β -scission rule, as assumed for the ortho quinolyl radical.

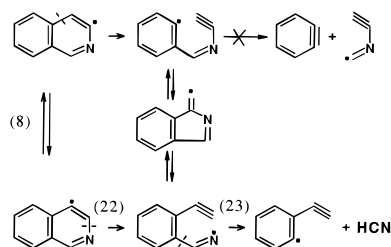


Figure 7. The reaction scheme showing the coupling between β -ortho and meta isoquinolyl and their reaction products. Numbers in parentheses indicate reaction numbers as they appear in the reaction scheme.

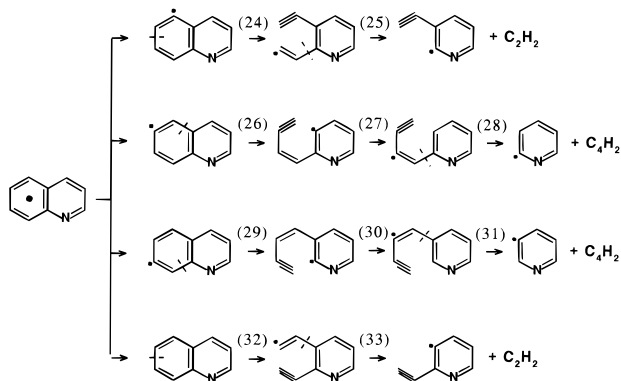


Figure 8. Four reaction pathways in the decomposition of quinolyl with the radical sites on the benzene ring. Numbers in parentheses indicate reaction numbers as they appear in the reaction scheme.

As can be seen in Figure 6, the open-chain radicals obtained by β -scissions in the meta and para quinolyl radicals can also undergo radical-induced cyclization \leftrightarrow decyclization reactions similar to the mechanism shown in Figure 5 and thus again couple the two pathways shown in Figure 6. There is, however, a marked difference in the nature of the coupling between the two pairs of pathways that expresses itself by the different locations of the nitrogen atom in the intermediate species. In the “preferred” pathway starting with the ortho radicals (Figure 5), the nitrogen atom in the intermediate specie is located outside the ring. It can undergo two different β -scissions. The specific bond cleavage and the consequent recyclization determines whether the final product is quinolyl or isoquinolyl. The coupling is thus between the quinoline and isoquinoline pathways. In the pathways of the meta and para quinolyl radicals, on the other hand (Figure 6), the nitrogen atom in the intermediate is part of the ring. It can also undergo two different β -scissions, but none of which changes the relative position of the nitrogen atom with respect to the benzene ring. Therefore, the specific bond cleavage in this intermediate and the consequent cyclization determines whether the final product is meta or para quinolyl and not whether it is quinolyl or isoquinolyl. The crossing from quinoline to isoquinoline and vice versa can take place in the ortho radicals *only*. Since it is believed that there is a fast equilibration of meta and para quinolyl radicals, the coupling of the two pathways shown in Figure 6 and the intermediate is insignificant from kinetic viewpoint. It was therefore not included in the reaction scheme.

Three isoquinolyl radicals are formed by removal of a hydrogen atom from the pyridine ring, α -ortho, β -ortho, and meta. Figure 5 shows the pathway for the α -ortho isoquinolyl radical, Figure 7 shows the pathways for the β -ortho and the meta radicals. The pathways of these two radicals are also coupled by an intermediate. However, the two possible β -scissions of the β -ortho isoquinolyl radical both lead to dead ends. One leads to formation of benzyne and isocyanide radical,

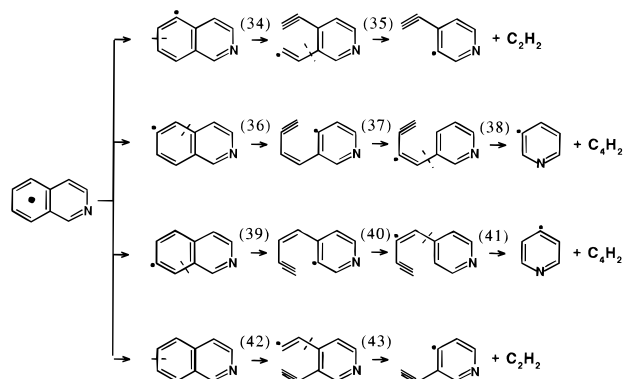


Figure 9. Four reaction pathways in the decomposition of isoquinolyl with the radical sites on the benzene ring. Numbers in parentheses indicate reaction numbers as they appear in the reaction scheme.

which is highly endothermic (~ 120 kcal/mol), and the second leads to the destruction of the resonance of the benzene ring owing to the formation of a C=C bond adjacent to the ring. Thus, decomposition of the β -ortho isoquinolyl radical was not included in the reaction scheme, its only reaction being its equilibration with the meta radical.

Figures 8 and 9 show the decomposition channels of the four different radical sites in quinoline and isoquinoline arising from removal of a hydrogen atom from the benzene ring. As has been mentioned before, since all C–H bonds in the benzene ring are of the same energy (~ 112 kcal/mol), we used a single radical in each isomer without specifying the radical site. Nonetheless, we examined the routes of all four possibilities in each isomer. Formation of C_4H_2 can be accounted for only by decomposition from radicals obtained by removal of a hydrogen atom from the benzene ring, as shown later when we discuss the computer modeling results.

2. Computer Modeling. A. Reaction Scheme. To account for the distribution of reaction products in the decomposition of both quinoline and isoquinoline, a common reaction scheme containing 72 species and 148 elementary reactions was composed (Table 3).

The Arrhenius parameters for the majority of the reactions were estimated by comparison with similar reactions with known rate parameters. Additional ones were taken from kinetic schemes that describe the decomposition mechanisms of benzene,^{9,16} benzonitrile,¹⁴ phenyl acetylene,¹⁷ and pyridine.¹⁰ Several parameters were taken from the NIST Chemical Kinetic Data Base.¹⁸

Thermodynamic properties of most the species were taken from literature sources.^{7,10,12,19,20} The heats of formation of several species were estimated using the NIST Structures and Properties program.⁵

B. Comparison of Model Calculations and Experimental Results. Figures 10–13 show the experimental and calculated mole percents of the four products formed in the “preferred” decomposition pathways (Figure 5), acetylene, cyanoacetylene, benzene, and benzonitrile. The filled squares (■) are the experimental points obtained with isoquinoline as a reactant and the open squares (□) with quinoline. The lines represent calculated mole percents at 25 K intervals. The solid lines are the model calculations for isoquinoline and the dashed lines for quinoline. In all of the four figures, the upper part A shows the calculations without the coupling of the quinoline and isoquinoline pathways (Figure 5), namely, with reactions 14 and 15 removed from the scheme. The lower part of the figures B shows the results of the calculations with the coupling.

TABLE 3: Reaction Scheme for the Decomposition of Quinoline and Isoquinoline^a (Values Are Given at 1400 K)

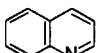
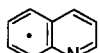
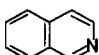
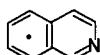
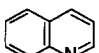
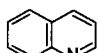
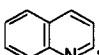
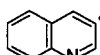
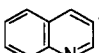
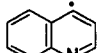
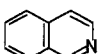
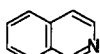
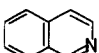
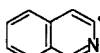
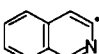
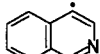
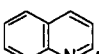
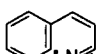
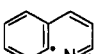
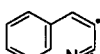
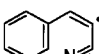
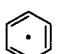
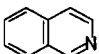
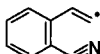
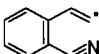
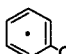
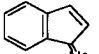
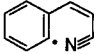
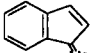
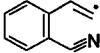
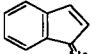
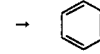
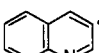
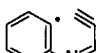
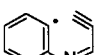
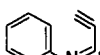
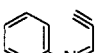

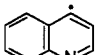
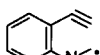
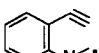
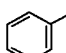
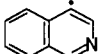
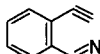
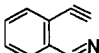
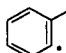
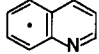
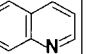
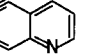
	Reaction	<i>A</i>	<i>E_a</i>	ΔS_r°	ΔH_r°	Source
1 ^b .	 →  + H [•]	8×10 ¹⁵	106	34	111	est ^c .
2 ^b .	 →  + H [•]	8×10 ¹⁵	106	34	111	est ^c .
3.	 →  + H [•]	6×10 ¹⁵	98	30	105	est ^d .
4 ^k .	 → 	1×10 ¹³	20	2	7	est.
5 ^k .	 → 	1×10 ¹³	15	0	-2	est.
6.	 →  + H [•]	3×10 ¹⁵	98	30	106	est ^d .
7.	 →  + H [•]	3×10 ¹⁵	98	30	105	est ^d .
8 ^k .	 → 	1×10 ¹³	15	0	-6	est.
9.	 → 	1×10 ¹⁴	35	12	24	est ^e .
10.	 → 	1×10 ¹³	25	0	0	est.
11 ^b .	 →  + HC≡CCN	1×10 ¹⁴	43	35	43	est.
12.	 → 	1×10 ¹⁴	35	16	22	est ^e .
13 ^b .	 →  + C ₂ H ₂	1×10 ¹⁴	43	37	43	est.
14.	 → 	1×10 ¹⁴	25	10	12	est.
15.	 → 	1×10 ¹⁴	25	13	9	est.
16.	 + H [•] → 	1×10 ¹⁴	0	-33	-97	est.
17.	 → 	1×10 ¹⁴	58	10	54	est ^f .
18.	 → 	1×10 ¹³	25	0	-6	est.
19 ^b .	 →  + HC≡CCN	1×10 ¹⁴	13	35	13	est.
20.	 → 	1×10 ¹⁴	46	10	43	est ^f .
21.	 →  + HCN	1×10 ¹⁴	16	38	16	est.
22.	 → 	1×10 ¹⁴	40	12	31	est ^f .
23.	 →  + HCN	1×10 ¹⁴	30	38	30	est.
24 ^b .	 →  → 	1×10 ¹⁴	58	12	53	est ^f .

TABLE 3: (Continued)

	Reaction	<i>A</i>	<i>E_a</i>	ΔS_r°	ΔH_r°	Source
25.		1×10^{14}	36	32	36	est.
26 ^b .		1×10^{14}	58	10	54	est ^f .
27.		1×10^{13}	25	0	0	est.
28.		1×10^{14}	30	43	29	est.
29 ^b .		1×10^{14}	52	10	48	est ^f .
30.		1×10^{13}	25	0	6	est.
31.		1×10^{14}	36	42	34	est.
32 ^b .		1×10^{14}	58	15	55	est ^f .
33.		1×10^{14}	44	34	44	est.
34 ^b .		1×10^{14}	62	13	56	est ^f .
35.		1×10^{13}	44	36	44	est.
36 ^b .		1×10^{14}	60	13	59	est ^f .
37.		1×10^{13}	25	0	0	est.
38.		1×10^{14}	32	39	30	est.
39 ^b .		1×10^{14}	60	13	58	est ^f .
40.		1×10^{13}	25	0	0	est.
41.		1×10^{14}	32	39	30	est.
42 ^b .		1×10^{14}	62	13	56	est ^f .
43.		1×10^{14}	44	36	44	est.
44.		1.5×10^{14}	13	3	-2	est ^g .
45 ^b .		5×10^{12}	12.5	-5	-8	est ^h .
46 ^b .		3×10^{12}	12.5	-4	-7	est ^h .
47 ^b .		5×10^{12}	12.5	-3	-8	est ^h .
48.		3×10^{12}	13	0	-2	est ^h .

TABLE 3: (Continued)

	Reaction	<i>A</i>	<i>E_a</i>	ΔS_r°	ΔH_r°	Source
49.		3×10^{12}	13	-3	-5	est ^h .
50.		3×10^{12}	13	-3	-6	est ^h .
51.		3×10^{12}	13	-3	-1	est ^h .
52.		5×10^{11}	12.5	1	-1	est.
53.		5×10^{11}	12.5	0	0	est.
54.		5×10^{11}	18	-3	8	est.
55 ^b .		1.5×10^{14}	16	6	4	est ^g .
56 ^b .		5×10^{12}	15	-1	-2	est ^h .
57 ^b .		3×10^{12}	15	-1	-1	est ^h .
58 ^b .		5×10^{12}	15	1	-2	est ^h .
59.		3×10^{12}	15	3	4	est ^h .
60.		3×10^{12}	15	0	1	est ^h .
61.		3×10^{12}	15	0	0	est ^h .
62.		3×10^{12}	15	0	5	est ^h .
63.		3×10^{11}	15	4	5	est.
64.		3×10^{11}	15	4	6	est.
65.		3×10^{11}	22	1	14	est.
66.		8×10^{13}	13	2	-1	est ^g .
67 ^b .		2.5×10^{12}	12.5	-5	-6	est ^h .
68 ^b .		1.5×10^{12}	12.5	-5	-6	est ^h .
69 ^b .		2.5×10^{12}	12.5	-3	-7	est ^h .
70.		1.5×10^{12}	13	-4	-9	est ^h .
71.		1.5×10^{12}	13	-6	-9	est ^h .
72.		1.5×10^{12}	13	-4	-5	est ^h .

TABLE 3: (Continued)

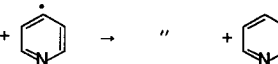
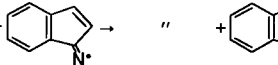
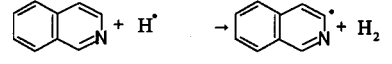
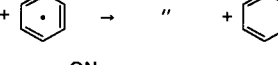
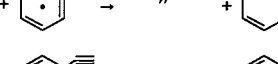
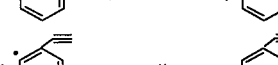

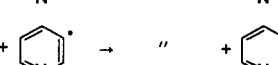
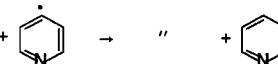
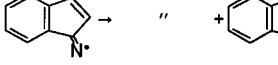
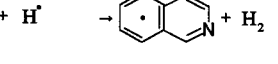
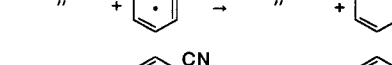
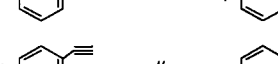
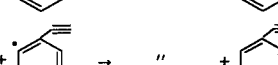
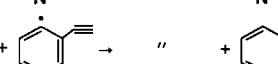
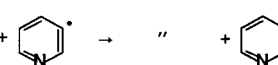
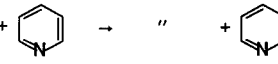
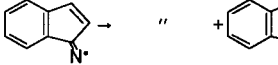
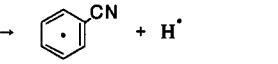
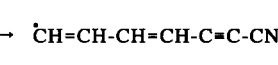
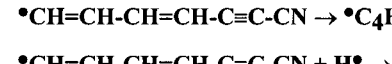

	Reaction	A	E_a	ΔS_r°	ΔH_r°	Source
73.		1.5×10^{12}	13	-4	-5	est ^h .
74.		1.5×10^{11}	18	-3	9	est.
75.		8×10^{13}	13	2	-3	est ^g .
76 ^b .		2.5×10^{12}	12.5	-5	-8	est ^h .
77 ^b .		1.5×10^{12}	12.5	-4	-8	est ^h .
78 ^b .		2.5×10^{12}	12.5	-3	-8	est ^h .
79.		1.5×10^{12}	13	-3	-11	est ^h .
80.		1.5×10^{12}	13	-5	-11	est ^h .
81.		1.5×10^{12}	13	-4	-7	est ^h .
82.		1.5×10^{12}	13	-4	-7	est ^h .
83.		1.5×10^{11}	18	-3	8	est.
84 ^b .		1.5×10^{14}	16	6	4	est ^g .
85 ^b .		5×10^{12}	15	-1	-1	est ^h .
86 ^b .		3×10^{12}	15	-1	-1	est ^h .
87 ^b .		5×10^{12}	15	1	-2	est ^h .
88.		3×10^{12}	15	0	-4	est ^h .
89.		3×10^{12}	15	-1	-4	est ^h .
90.		3×10^{12}	15	0	-3	est ^h .
91.		3×10^{12}	15	0	-3	est ^h .
92.		1.5×10^{11}	22	1	15	est.
93 ^b .		7.6×10^{15}	106	35	112	14.
94 ^b .		1×10^{14}	67	14	64	14.
95.	$\bullet\text{CH}=\text{CH}-\text{CH}=\text{CH}-\text{C}\equiv\text{C}-\text{CN} \rightarrow \bullet\text{C}_4\text{H}_3 + \text{HCCCN}$	2×10^{14}	41	34	44	14.
96.	$\bullet\text{CH}=\text{CH}-\text{CH}=\text{CH}-\text{C}\equiv\text{C}-\text{CN} + \text{H}\bullet \rightarrow l\text{-C}_6\text{H}_4 + \text{HCN}$	5×10^{14}	4	4	-71	14

TABLE 3: (Continued)

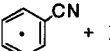
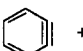
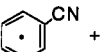
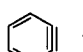
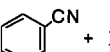
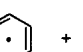
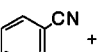
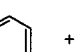
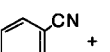
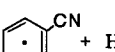
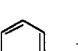

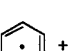
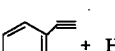
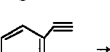
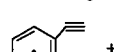
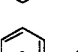
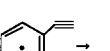
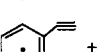
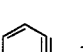
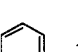
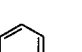
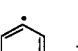
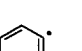
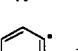
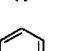
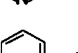
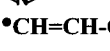
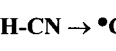
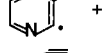
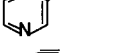
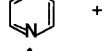
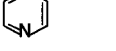
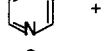
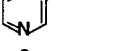
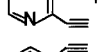
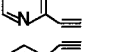
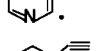
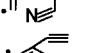

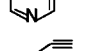
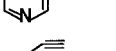
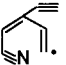
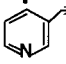
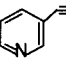
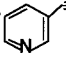
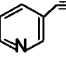
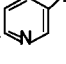
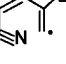
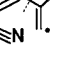
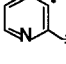
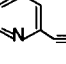
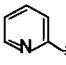
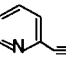
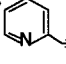
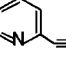
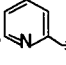
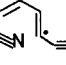
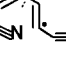
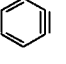
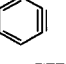
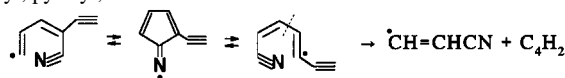
	Reaction	A	E_a	ΔS_r°	ΔH_r°	Source
97 ^b .	 + H [•] →  + HCN	5×10 ¹⁴	0	5	−19	est.
98 ^b .	 + CN [•] →  + C ₂ N ₂	5×10 ¹³	0	−2	−2	est.
99 ^b .	 + H [•] →  + HCN	2×10 ¹⁴	12.6	7	2	14.
100.	 + H [•] →  + CN [•]	2×10 ¹⁴	19.0	2	16	14.
101 ^b .	 + H [•] →  + H ₂	1×10 ¹⁴	16.0	7	5	14.
102 ^b .	 →  + H [•]	8×10 ¹⁵	106	35	113	9, 18.
103 ^b .	 + C ₂ H ₂ →  + H [•]	3.6×10 ¹²	8.0	−8	−2	17.
104 ^b .	 →  + H [•]	5×10 ¹⁶	113.5	33	113	17.
105 ^b .	 → $\cdot\text{CH}=\text{CH}-\text{CH}=\text{CH}-\text{C}\equiv\text{CH}$	1×10 ¹⁴	67	10	65	9, 18.
106.	$\cdot\text{CH}=\text{CH}-\text{CH}=\text{CH}-\text{C}\equiv\text{CH} \rightarrow \cdot\text{C}_4\text{H}_3 + \text{C}_2\text{H}_2$	1×10 ¹⁴	40	42	39	9, 21.
107 ^b .	 → $\cdot\text{CH}=\text{CH}-\text{CH}=\text{CH}-\text{C}\equiv\text{C}-\text{C}\equiv\text{CH}$	1×10 ¹⁴	67	15	65	est. ^f .
108 ^b .	 + H [•] →  + C ₂ H ₂	1×10 ¹⁴	0	7	−20	est.
109.	$\cdot\text{CH}=\text{CH}-\text{CH}=\text{CH}-\text{C}\equiv\text{C}-\text{C}\equiv\text{CH} \rightarrow \cdot\text{C}_4\text{H}_3 + \text{C}_4\text{H}_2$	1×10 ¹⁴	40	40	42	est.
110.	 →  + H [•]	8×10 ¹⁵	98	34	106	10.
111 ^k .	 → 	1×10 ¹³	15	0	0	est.
112 ^k .	 → 	1×10 ¹³	15	0	−6	est.
113.	 → $\cdot\text{CH}=\text{CH}-\text{CH}=\text{CH}-\text{CN}$	1×10 ¹⁴	35	10	24	10, 12.
114.	$\cdot\text{CH}=\text{CH}-\text{CH}=\text{CH}-\text{CN} \rightarrow \cdot\text{CH}=\text{CHCN} + \text{C}_2\text{H}_2$	1×10 ¹⁴	52	35	52	est, 10
115.	 + H [•] → 	2×10 ¹³	0	−30	−107	est.
116.	 + H [•] → 	2×10 ¹³	0	−30	−113	est.
117.	 + H [•] → 	2×10 ¹³	0	−35	−113	est.
118.	 + H [•] → 	2×10 ¹³	0	−33	−113	est.
119.	 → 	1×10 ¹⁴	35	16	24	est. ^e .
120 ⁱ .	 → $\cdot\text{CH}=\text{CHCN} + \text{C}_4\text{H}_2$	1×10 ¹⁴	45	38	44	est.
121 ^k .	 → 	1×10 ¹³	15	0	−6	est.
122.	 → 	1×10 ¹⁴	35	16	24	est. ^e .

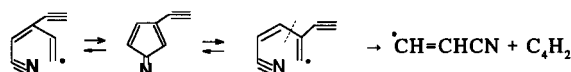
TABLE 3: (Continued)

	Reaction	A	E_a	ΔS_r°	ΔH_r°	Source
123 ^j .	 $\rightarrow \cdot\text{CH}=\text{CHCN} + \text{C}_4\text{H}_2$	1×10^{14}	45	38	44	est.
124 ^k .	 \rightarrow 	1×10^{13}	15	0	0	est.
125 ^k .	 \rightarrow 	1×10^{13}	15	0	-6	est.
126.	 \rightarrow 	1×10^{14}	35	16	24	est ^e .
127.	 $\rightarrow \cdot\text{CH}=\text{CHCN} + \text{C}_4\text{H}_2$	1×10^{14}	45	38	44	est.
128 ^k .	 \rightarrow 	1×10^{13}	15	0	0	est.
129 ^k .	 \rightarrow 	1×10^{13}	15	0	0	est.
130 ^k .	 \rightarrow 	1×10^{13}	15	0	-6	est.
131.	 \rightarrow 	1×10^{14}	35	16	24	est ^e .
132.	 $\rightarrow \cdot\text{CH}=\text{CHCN} + \text{C}_4\text{H}_2$	1×10^{14}	45	38	44	est.
133.	$\cdot\text{CH}=\text{CHCN} \rightarrow \text{HCCCN} + \text{H}^\bullet$	1×10^{14}	50	24	49	est, 10.
134.	$\cdot\text{CH}=\text{CHCN} \rightarrow \text{C}_2\text{H}_2 + \text{CN}^\bullet$	1×10^{14}	61	31	62	est, 10.
135.	$\cdot\text{CH}=\text{CHCN} + \text{H}^\bullet \rightarrow \text{C}_2\text{H}_3\text{CN}$	1×10^{14}	0	-31	-108	est, 10.
136.	$\cdot\text{CH}=\text{CHCN} + \text{H}^\bullet \rightarrow \text{C}_2\text{H}_2 + \text{HCN}$	1×10^{14}	0	1.1	-65	est, 10.
137.	 $\rightarrow \text{CH}=\text{C}-\text{CH}=\text{CH}-\text{C}=\text{CH}$	5×10^{13}	40	13	12	est.
138.	$\text{C}_4\text{H}_3^\bullet + \text{C}_2\text{H}_2 \rightarrow$  $+ \text{H}^\bullet$	$4.9 \times 10^{-32} T^{11.47}$	2.3	-20	-13	20.
139.	$\text{C}_4\text{H}_3^\bullet + \text{C}_2\text{H}_2 \rightarrow \text{CH}=\text{C}-\text{CH}=\text{CH}-\text{C}=\text{CH} + \text{H}^\bullet$	$1.7 \times 10^{-5} T^{4.44}$	6.9	-7	-2	20.
140.	$\text{C}_4\text{H}_3^\bullet \rightarrow \text{C}_4\text{H}_2 + \text{H}^\bullet$	1.1×10^{14}	39	25	40	23, 24.
141.	$\text{C}_4\text{H}_3^\bullet \rightarrow \text{C}_2\text{H}_2 + \text{C}_2\text{H}^\bullet$	1×10^{14}	60	29	58	est, 9.
142.	$\text{C}_4\text{H}_3^\bullet + \text{H}^\bullet \rightarrow \text{C}_2\text{H}_2 + \text{C}_2\text{H}_2$	1×10^{14}	0	-3	-72	est, 25
143.	$\text{C}_4\text{H}_3^\bullet + \text{H}^\bullet \rightarrow \text{C}_4\text{H}_2 + \text{H}_2$	8.13×10^{13}	0	-3	-67	18.
144.	$\text{C}_2\text{H}^\bullet + \text{HCN} \rightarrow \text{HCCCN} + \text{H}^\bullet$	2×10^{12}	0	-9	-17	est, 10.
145.	$\text{C}_2\text{H}^\bullet + \text{HCCCN} \rightarrow \text{C}_4\text{H}_2 + \text{CN}^\bullet$	7×10^{12}	3.0	3	-5	est, 10.
146.	$\text{C}_2\text{H}_2 + \text{C}_2\text{H}^\bullet \rightarrow \text{C}_4\text{H}_2 + \text{H}^\bullet$	1.3×10^{13}	0.0	-4	-18	26.
147.	$\text{H}_2 + \text{Ar} \rightarrow \text{H}^\bullet + \text{H}^\bullet$	1.4×10^{15}	101.4	28	107	18.
148.	$\text{C}_2\text{H}_2 + \text{Ar} \rightarrow \text{C}_2\text{H}^\bullet + \text{H}^\bullet + \text{Ar}$	3.8×10^{16}	107.0	32	130	18.

^a ΔH_r° and ΔS_r° are expressed in units of kcal/mol and cal/(K mol), respectively. Rate constants are expressed as $k = A \exp(-E_a/RT)$ in units of cm^3 , s, mol, kcal. ^b The point in the middle of the ring means that the corresponding radical was introduced into the reaction scheme in "common" form, namely, irrespective of its exact location on the ring. ^c Estimation based on H-atom ejection from benzene (ref 18). ^d Estimation based on H-atom ejection from ortho position in pyridine (ref 10). ^e Estimation based on rupture of ortho pyridyl radical (refs 10 and 12). ^f Estimation based on rupture of phenyl radical (refs 9, 18, and 21) with respect to the corresponding reaction thermochemistry. ^g Estimation based on H-atom abstraction from benzene (refs 9 and 16) and pyridine (ref 10) rings. ^h H-atom abstraction from aromatic molecules by phenyl were reported in the work of Fahr and Stein;²² such abstractions by phenyl, pyridyl, and their derivatives are also introduced into the reaction scheme. ⁱ Reaction is not elementary:



^j Reaction is not elementary:



^k Reaction is not elementary, see text (Discussion, part 1A.).

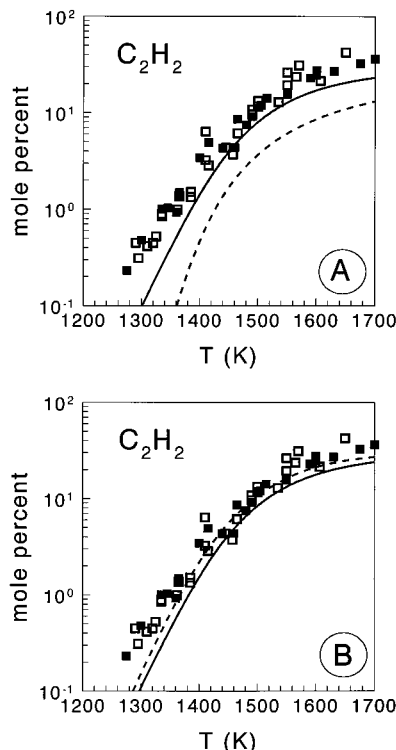


Figure 10. Comparison between experimental and calculated mole percent of acetylene. \square and broken line, quinoline; \blacksquare and solid line, isoquinoline. The upper part (A) shows results of model calculations without coupling between quinoline and isoquinoline (Figure 5). The lower part (B) shows the results with coupling.

As can readily be seen, as expected, without the coupling of two pathways shown in Figure 5, the calculated product distributions are different for the two isomers. On the other hand, when the two pathways are coupled the agreement with experiment (in the sense that both quinoline and isoquinoline show almost identical distribution of reaction products) is very good. The effect of coupling is particularly pronounced in benzonitrile, as the α -ortho radical pathway in isoquinoline is the only route by which benzonitrile can be formed when quinoline is the starting material. It is less pronounced in the other three products, as they are also produced by other channels, in which this coupling does not play any role.

Figures 14–16 show the experimental and calculated results for diacetylene, hydrogen cyanide, and phenyl acetylene. These products are formed via other reaction channels, and the coupling of the ortho radical pathways (Figure 5) affects their concentrations only very slightly. The symbols and the lines in the figures are the same as those in the previous four figures. The additional line at the bottom of Figure 14 shows the

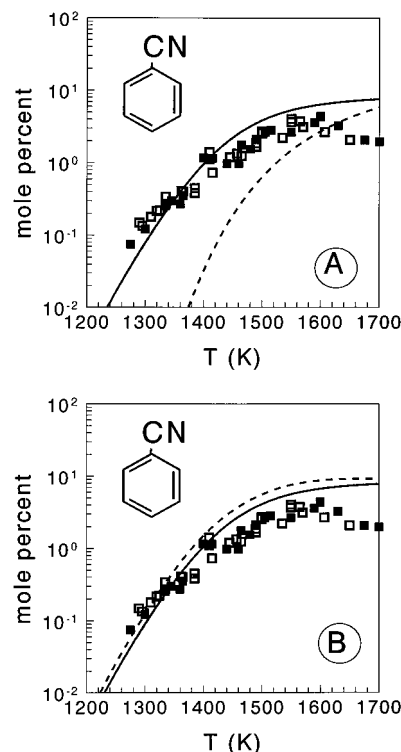


Figure 11. Comparison between experimental and calculated mole percent of benzonitrile. \square and broken line, quinoline; \blacksquare and solid line, isoquinoline. The upper part (A) shows results of model calculations without coupling between quinoline and isoquinoline (Figure 5). The lower part (B) shows the results with coupling.

calculated mole percent of diacetylene after eliminating all the reactions of quinolyl and isoquinolyl with the radical sites on the benzene ring. The diacetylene formed by reaction channels involving acetylene, such as $\text{C}_2\text{H}_2 + \text{C}_2\text{H}_2 \rightarrow \text{C}_4\text{H}_3^\bullet + \text{H}$ followed by $\text{C}_4\text{H}_3^\bullet \rightarrow \text{C}_4\text{H}_2 + \text{H}^\bullet$, are not fast enough at the temperatures of this study to account for the observed C_4H_2 . Figure 17 shows the overall decomposition of quinoline and isoquinoline.

C. Open Questions. There are still some open questions regarding the experimental results and the model calculations. 1. Why does the coupling between quinoline and isoquinoline not promote a quinoline \leftrightarrow isoquinoline isomerization? 2. Why were indene imine and other intermediates not identified in the postshock mixtures? 3. If the reactions of quinolyl and isoquinolyl with radical sites on the benzene ring are responsible for the production of diacetylene (Figures 8 and 9), why are pyridine and pyridyl acetylene formed in these reactions absent from the products?

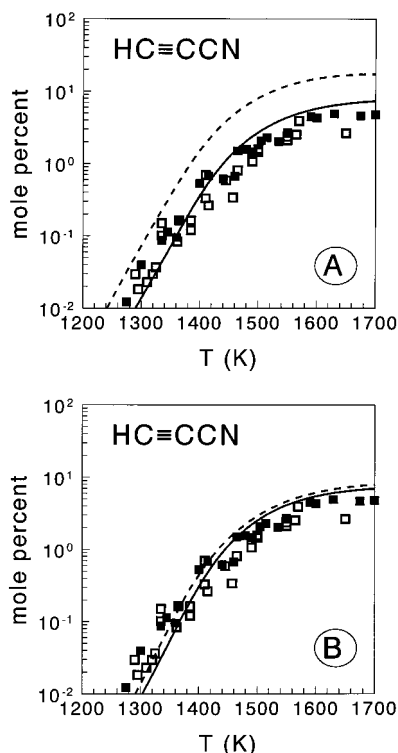


Figure 12. Comparison between experimental and calculated mole percent of cyano acetylene. \square and broken line, quinoline; \blacksquare and solid line, isoquinoline. The upper part (A) shows results of model calculations without coupling between quinoline and isoquinoline (Figure 5). The lower part (B) shows the results with coupling.

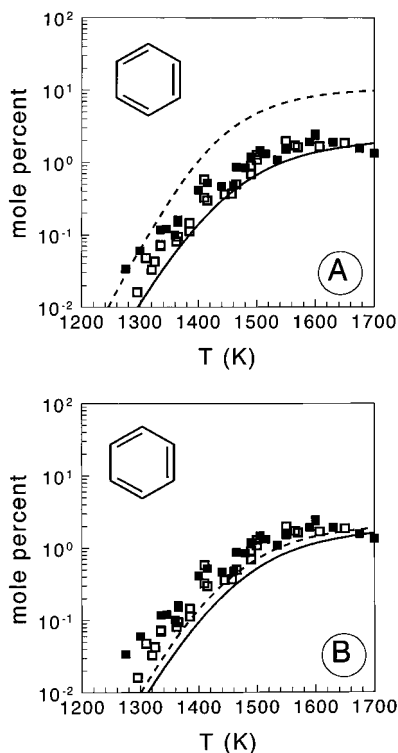


Figure 13. Comparison between experimental and calculated mole percent of benzene. \square and broken line, quinoline; \blacksquare and solid line, isoquinoline. The upper part (A) shows results of model calculations without coupling between quinoline and isoquinoline (Figure 5). The lower part (B) shows the results with coupling.

Figure 18 shows the calculated mole percent of isoquinoline in tests with quinoline as the reactant. The calculations show

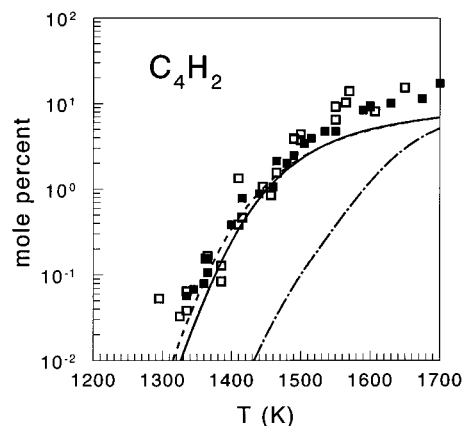


Figure 14. Comparison between experimental and calculated mole percent of diacetylene. \square and broken line, quinoline; \blacksquare and solid line, isoquinoline. The lower broken line shows the model calculations where all the reactions in the two schemes shown in Figures 8 and 9 are removed from the overall reaction scheme. Production of diacetylene by reactions of acetylene alone cannot account for its observed mole percent.

that its mole percent is around 1×10^{-3} , below the detection limit. This observation is somewhat surprising. The coupling mechanism shown in Figure 5 should have led to a quinoline isoquinoline isomerization since the open-chain radical coming from β -scission of the ortho quinolyl exchanges to the equivalent radical in isoquinoline. Cyclization of the latter and recombination with a hydrogen atom (or abstraction of one) should lead to isomerization.

This discrepancy can be clarified by examining the competition between the two parallel reactions of the open-chain radicals, fragmentation on one hand, and cyclization followed by H-atom recombination on the other hand.

Since the cyclization–decyclization processes of the radicals are very fast at the temperature range of the present investigation, the species involved in these processes are effectively equilibrated. The rate of formation of isoquinoline in tests where quinoline is the reactant is thus given by (see Figure 5)

$$\frac{d[\text{isoquinoline}]}{dt} = \underbrace{\frac{k_{-12}}{k_{12}} \{k_{-6}[\text{H}^*] + (k_{62} + k_{63})[\text{quinoline}]\}}_{k_{\text{isoquinoline}}} \left[\text{quinolyl radical} \right]$$

where

$$\frac{k_{-12}}{k_{12}} \left[\text{quinolyl radical} \right] = \left[\text{isoquinolyl radical} \right]$$

The two terms in the curled parenthesis represent the rates of recombination with and abstraction of hydrogen atoms. The fragmentation rate of the open-chain radical to acetylene and benzonitrile radical is

$$\frac{d[\text{C}_2\text{H}_2]}{dt} = k_{13} \left[\text{quinolyl radical} \right]$$

The computer simulation shows that the ratio $k_{13}/k_{\text{isoquinoline}}$ is around 3×10^3 at 1300 K and 8×10^3 at 1550 K. This result is due to the very low concentration of hydrogen atoms and a very low rate of abstraction by large radical species.

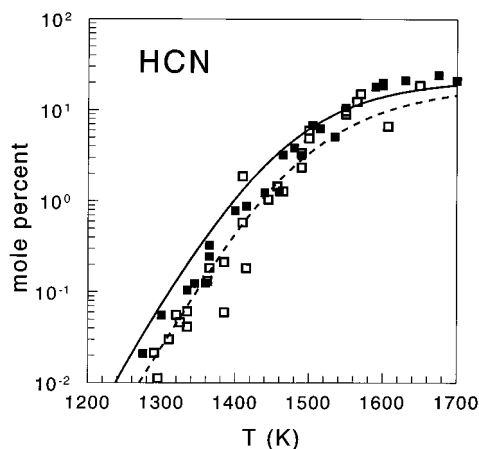


Figure 15. Comparison between experimental and calculated mole percent of hydrogen cyanide. \square and broken line, quinoline; \blacksquare and solid line, isoquinoline. The modeling is done with coupling.

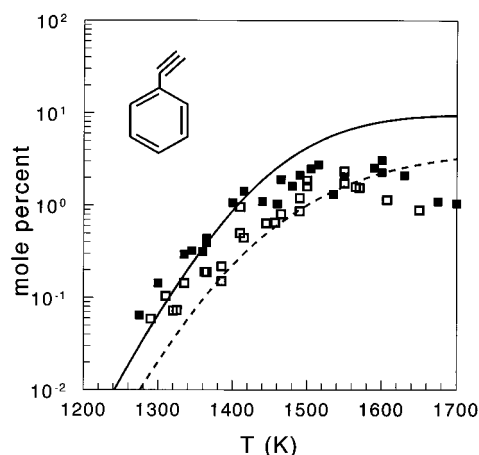


Figure 16. Comparison between experimental and calculated mole percent of phenyl acetylene. \square and broken line, quinoline; \blacksquare and solid line, isoquinoline. A slight difference in the mole percent of phenyl acetylene in decomposition of quinoline and isoquinoline is seen in both the experiment and the calculations. The modeling is done with coupling.

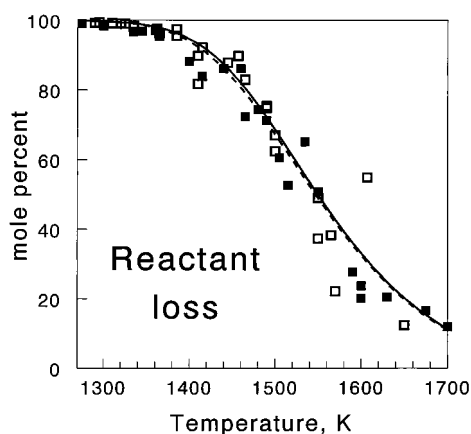


Figure 17. Comparison between experimental and calculated mole percent of reactant loss. \square and broken line, quinoline; \blacksquare and solid line, isoquinoline.

The considerations regarding our ability to identify the intermediate indene imine in the postshock mixtures are similar to those of indentifying isoquinoline. The computations show that not only the abstraction of hydrogen atoms from quinoline by indene imine radical is very slow (it is endothermic by 8–14

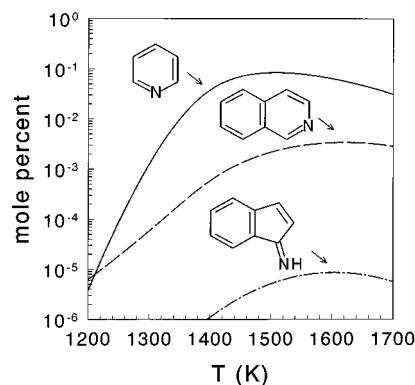


Figure 18. Calculated mole percent of pyridine, isoquinoline and the indene imine intermediate with quinoline as the decomposing compound. The mole percents of all the three compounds are very small; for two, they are below the detection limit. Pyridine was identified in the postshock mixtures but in minute quantities that did not allow a quantitative analysis.

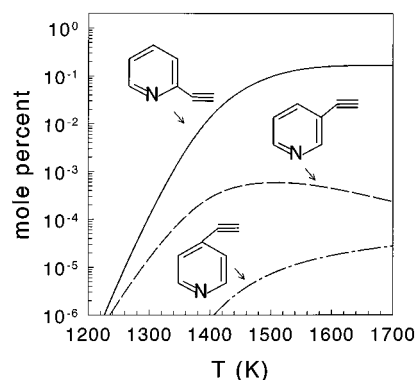


Figure 19. Calculated mole percents of ortho, meta, and para pyridyl acetylene. Pyridyl acetylene was identified in the postshock mixtures but in minute quantities that did not allow a quantitative analysis.

kcal/mol) but also its equilibrium concentration is extremely small. The expected mole percent of indene imine is very low and practically unrecoverable, as can be seen in Figure 18.

The two pairs of products, diacetylene and pyridyl radical and acetylene and pyridyl acetylene radical, are formed in the process of opening the benzene ring in both quinoline and isoquinoline. On the other hand, opening of the pyridine ring, in the main channel, leads to the production of phenyl and cyanoacetylene and to benzonitrile radical and acetylene. Whereas phenyl and benzonitrile radicals show up as benzene and benzonitrile in the line of the products, pyridine and pyridyl acetylene were identified only in minute quantities. The reason for this behavior is the very low stability of pyridyl and pyridyl acetylene radicals as compared to phenyl and benzonitrile radicals, which do not have a nitrogen atom in the ring. The decomposition of pyridyl requires only 35 kcal/mol,¹² whereas the decomposition of phenyl requires some 65 kcal/mol.⁹ Pyridyl decomposes almost completely before it has the chance to recombine or to abstract a hydrogen atom, whereas phenyl and benzonitrile radicals are stable enough and have a long enough lifetime to recombine or to abstract a hydrogen atom from the reactant.

Figures 18–19 show calculated yields of pyridine, ortho, meta, and para pyridyl acetylenes produced according to the present scheme from quinoline as a reactant. As can be seen, only pyridine and ortho pyridyl acetylene are expected to be produced in detectable amounts. Compounds having $m/z = 79$

TABLE 4: Sensitivity Factors $S_{ij} = \Delta \log C_i / \Delta \log k_i$ at 1300/1550 K for Quinoline. k Is Changed by a Factor of 3

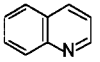
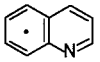
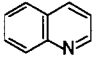
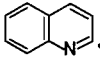
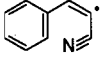
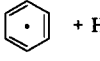
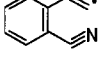
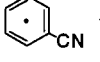
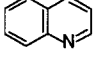
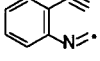
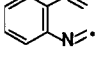
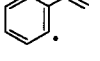
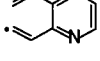
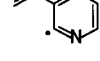
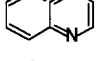
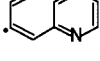
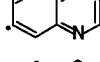
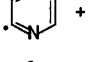
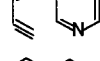
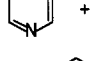
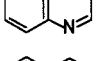
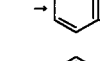
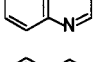
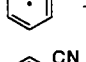
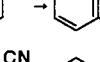
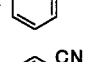
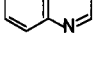
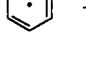
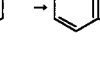
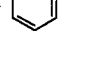
N°	Reaction	C ₂ H ₂	C ₆ H ₅ CN	HCCCN	C ₆ H ₆	HCN	C ₆ H ₅ -C ₂ H	C ₄ H ₂
1.	 →  + H [•]							0.11 / --
3.	 →  + H [•]	0.88 / 0.42	0.87 / 0.40	0.87 / 0.22	0.89 / 0.42	0.99 / 0.62	0.88 / 0.57	0.80 / 0.11
11.	 →  + HC≡CCN			0.77 / 0.25	0.89 / 0.64			
13.	 →  + C ₂ H ₂	0.10 / --	0.10 / --	-0.61 / -0.13	-0.86 / -0.48	-0.61 / --	-0.82 / -0.48	
20.	 → 					0.20 / --	0.23 / 0.31	
21.	 →  + HCN					0.38 / --	0.44 / 0.22	
25.	 →  + C ₂ H ₂			0.20 / --				0.51 / --
27.	 → 							0.51 / --
28.	 →  + C ₄ H ₂							0.16 / --
31.	 →  + C ₄ H ₂							0.18 / --
44.	 + H [•] →  + H ₂	0.11 / 0.17	0.11 / 0.32	0.11 / 0.17	0.11 / 0.11		0.11 / 0.29	-- / 0.15
45.	 +  →  + 				0.11 / 0.17			
46.	 +  →  + 	0.55 / 0.21	0.69 / 0.48	0.47 / --	0.55 / 0.25	0.47 / --	0.55 / 0.31	

TABLE 4 (Continued)

47.						0.11 / --	
55.						-0.12 / --	0.17 / 0.29
57.						-0.19 / --	0.36 / 0.29
93.						-- / -0.24	-- / -0.11
97.						0.16 / 0.18	-- / -0.20
99.						-- / 0.11	-- / -0.14
103.						-- / -0.14	-- / 0.15

and 103 corresponding to pyridine and pyridyl acetylene were indeed identified in the postshock mixtures, but only in trace amounts that could not be analyzed quantitatively.

D. Sensitivity Analysis. Table 4 shows the sensitivity spectrum of the reaction scheme for the decomposition of quinoline as the reactant, at 1300 and 1500 K. The sensitivity factor $S_{i,j}$ is defined in the table as: $\Delta \log C_i / \Delta \log k_j$ at 2 ms. It was evaluated here by changing k_j by a factor of 3. ($S_{i,j} = 1$ means that a factor of 3 change in k_j causes a factor of 3 change in C_i .) Reactions for which $S_{i,j}$ is less than 0.1 for all the products both at low and high temperatures are not included in the table. The sensitivity spectrum for the decomposition of isoquinoline is practically identical in its context to that of quinoline and it is thus not shown.

Most of the features in the sensitivity spectrum are self-evident. It is of interest, however, to examine some of the details in the mechanism in light of the information given in Table 4. Since the overall mechanism of the decomposition of quinoline is essentially a free radical mechanism, ejection of a hydrogen atom from the molecule, being the initiation step, is a very important step to which the entire system is very sensitive. However, since ejection of H atom from the ortho position in the pyridine ring (reaction 3) is faster than ejection of H from other sites in the pyridine and benzene rings, the contribution of reaction 1, for example, to the concentration of H atoms in the system is no more than 5–7% and does not affect the product concentrations.

Although diacetylene (C_4H_2) is a direct product of the quinolyl radical which is formed in reaction 1, its formation is more sensitive to the value of k_3 than to the value of k_1 . The reason for this is that reaction 55, which also produces quinolyl with the radical site on the benzene ring, depends on the total concentration of H atoms which is determined mainly by the rate of reaction 3. Indeed, as can be seen in Table 4, diacetylene production is sensitive to reaction 55 with roughly the same sensitivity factor as reaction 1.

Another interesting feature is the competition between the decomposition channels of the two open-chain radicals at the two ends of the indene imine radical, (i.e., reactions 11 and 13). Reaction 13, which is responsible for the formation of acetylene and benzonitrile, strongly inhibits the products of the second open-chain radical (reaction 11). Since cyclization \leftrightarrow decyclization of indene imine radical is fast, the three radicals involved are practically in equilibrium with one another, and increasing or decreasing the rate of these processes has no effect on the product distribution.

V. Conclusion

The mechanism of the thermal decomposition of quinoline and isoquinoline can be summarized as follows.

1. The decomposition is initiated by H-atom ejections from sites in both the pyridine and the benzene rings, with ejection from the ortho position relative to the nitrogen in the pyridine ring preferred.

2. The distribution of reaction products in quinoline is identical with that of isoquinoline even though the preferred decomposition routes in the two isomers are different.

3. An intermediate indene imine radical couples, in fast cyclization \leftrightarrow decyclization processes, the decomposition routes of the two isomers and is thus responsible for the identical product distributions.

4. A combined reaction scheme for quinoline and isoquinoline containing 72 species and 148 elementary reactions

successfully accounts for the product distribution as a function of temperature.

Acknowledgment. This research was supported by a grant from the Israel Coal Supply Co. The authors thank Professor J. A. Berson of Yale University for very helpful discussions.

References and Notes

- (1) Attar, A.; Hendrickson, G. G. In *Coal Structure*; Meyers, R. A., Ed.; Academic Press: New York, 1982; p 132.
- (2) Given, P. H. In *Coal Science*; Gorbaty, M. L., Larsen, J. W., Wender, I., Eds.; Academic Press: New York, 1982; Vol. 3, p 65.
- (3) Unsworth, J. F. In *Coal Quality and Combustion Performance*; Unsworth, J. F.; Barrat, D. J., Roberts, P. T., Eds.; Elsevier Science Publishers: Amsterdam, 1991; Chapter 4.2, p 206.
- (4) Laskin, A.; Lifshitz, A. *J. Phys. Chem. A* **1997**, *101*, 7787.
- (5) Lifshitz, A.; Tamburu, C.; Suslensky, A. *J. Phys. Chem.* **1989**, *93*, 5802.
- (6) Mackie, J. C.; Colket, M. B., III; Nelson, P. F.; Esler, M. *Int. J. Chem. Kinet.* **1991**, *23*, 733.
- (7) Stein, S. E.; Rukkers, J. M.; Brown, R. L. *NIST-Standard Reference Data Base 25*; National Institute of Standards and Technology: Washington, DC, 1993.
- (8) Bruinsma, O. S. L.; Tromp, P. J. J.; de Sauvage Nolting, H. J. J.; Moulijn, J. A. *Fuel* **1988**, *67*, 334.
- (9) Laskin, A.; Lifshitz, A. *Proceedings of the 26th International Symposium on Combustion*; The Combustion Institute: Pittsburgh, PA, 1996; p 669 and refs 1–11 cited therein.
- (10) Mackie, J. C.; Colket, M. B., III; Nelson, P. F. *J. Phys. Chem.* **1990**, *94*, 4099 and refs 6–10 cited therein.
- (11) Kern, R. D.; Xie, K. *Prog. Energy Combust. Sci.* **1991**, *17*, 191.
- (12) Jones, J.; Bacskay, G. B.; Mackie, J. M. *Isr. J. Chem.* **1996**, *36*, 239.
- (13) Lifshitz, A.; Tamburu, C.; Frank, P.; Just, Th. *J. Phys. Chem.* **1993**, *97*, 4085.
- (14) Lifshitz, A.; Cohen, Y.; Braun-Unkhoff, M.; Frank, P. *Proceedings of the 26th International Symposium on Combustion*; The Combustion Institute: Pittsburgh, PA, 1996; p 659.
- (15) Giese, B.; Kopping, B.; Göbel, T.; Dickhant, J.; Thoma, G.; Kulicke, K. J.; Trach, F. *Radical Cyclization Reactions. In Organic Reactions*; John Wiley and Sons: New York, 1996; Vol. 48, p 303.
- (16) Kiefer, J. H.; Mizerka, L. J.; Patel, M. R.; Wei, H. C. *J. Phys. Chem.* **1985**, *89*, 2013.
- (17) Hertzler, J.; Frank, P. *Ber. Bunsen-Ges. Phys. Chem.* **1992**, *96*, 1333.
- (18) Westly, F.; Herron, J. T.; Cvetanovich, R. J.; Hampson, R. F.; Mallard, W. G. *NIST-Chemical Kinetics Standard Reference Data Base 17*, Version 5.0, National Institute of Standards and Technology: Washington, DC, 1985.
- (19) Burcat, A.; McBride, B. *1995 Ideal Gas Thermodynamics Data for Combustion and Air-Pollution Use*; Technion—Israel Institute of Technology: Haifa, 1995. (TEA 732).
- (20) Wang, H.; Frenklach, M. *J. Phys. Chem.* **1994**, *98*, 11465.
- (21) Braun-Unkhoff, M.; Frank, P.; Just, Th. *Proceedings of the International 22th Symposium on Combustion*; The Combustion Institute: Pittsburgh, PA, 1988; p 1053.
- (22) Fahr, H.; Stein, S. E. *J. Phys. Chem.* **1988**, *92*, 4951.
- (23) Back, M. H. *Can. J. Chem.* **1971**, *49*, 2199.
- (24) Weissman, M.; Benson, S. W. *Int. J. Chem. Kinet.* **1984**, *16*, 307.
- (25) Benson, S. W. *Int. J. Chem. Kinet.* **1989**, *21*, 233.
- (26) Laufer, A. H.; Bass, A. M. *J. Phys. Chem.* **1979**, *83*, 310.
- (27) Number in parentheses indicates the number of the reaction in the kinetic scheme.